Self-consistent meson mass spectrum

Louis A. P. Balázs
Physics Department, Purdue University, West Lafayette, Indiana 47907
(Received 7 June 1982)

A dual-topological-unitarization (or dual-fragmentation) approach to the calculation of hadron masses is presented, in which the effect of planar "sea"-quark loops is taken into account from the beginning. Using techniques based on analyticity and generalized ladder-graph dynamics, we first derive the approximate "generic" Regge-trajectory formula $\alpha(t)=\max(S_1+S_2,S_3+S_4)-\frac{1}{2}+2\hat{\alpha}'[s_a+\frac{1}{2}(t-\sum m_i^2)]$ for any given hadronic process $1+2\to 3+4$, where S_i and m_i are the spins and masses of $i=1,2,3,4$, and $\sqrt{s_a}$ is the effective mass of the lowest nonvanishing contribution (a) exchanged in the crossed channel. By requiring a minimization of secondary (background, etc.) contributions to a, and demanding simultaneous consistency for entire sets of such processes, we are then able to calculate the masses of all the lowest pseudoscalar and vector $q\bar{q}$ states with $q=u,d,s$, and the Regge trajectories on which they lie. By making certain additional assumptions we are also able to do this with $q=u,d,c$ and $q=u,d,b$. Our only arbitrary parameters are m_ρ, m_{K^*}, m_ψ, and m_Υ, one of which merely serves to fix the energy scale. In contrast to many other approaches, a small m_π^2/m_ρ^2 ratio arises quite naturally in the present scheme.

I. INTRODUCTION

Calculations of the hadron mass spectrum can be divided into two basic types:

(A) Semiphenomenological, which depend wholly, or in part, on *ad hoc* phenomenological potentials or bag-boundary conditions parametrized by a number of arbitrary parameters which are fitted to the data. Most practical spectrum calculations have been of this type and have met with a certain degree of success, although a number of serious problems still remain.

(B) More fundamental. Some of these, such as the ones based on the QCD sum rules of Shifman, Vainshtein, and Zakharov,[1] while successful, are in principle only capable of giving a limited set of results. Of the ones which are theoretically capable of dynamically generating a complete spectrum, the lattice approach has recently received the most attention. Here the usual space-time continuum is replaced by a discrete grid and the light "sea" quarks are generally neglected as a first approximation. The latter assumption is sometimes justified on the basis of an $N_{\text{flavor}}/N_{\text{color}}\to 0$ limit of quantum chromodynamics (QCD). However, $N_{\text{flavor}}/N_{\text{color}}\sim 1$ in the real world and sea quarks are known to play an important role for small fractional quark momenta (x) within hadrons in deep-inelastic lepton-hadron scattering experiments. Since small x corresponds to the crucial long-range part of the confinement region, there is every reason to expect that a realistic spectrum will emerge only when the sea-quark loops of, e.g., Fig. 1, are properly taken into account. The usual difficulties in accounting for the smallness of the pion mass may be a manifestation of this fact.

The dual-topological-unitarization (DTU) program[2] is a highly promising fundamental approach to the confinement region in which sea quarks, and hence quark loops, are assumed to play an important role from the beginning. Instead of going to a lattice, one uses continuum-space techniques based on analyticity and unitarity—general properties which have been extensively tested for hadronic processes in the past. DTU methods have, of course, already seen many successful applications,[2] particularly in jet and cross-section physics.[3]

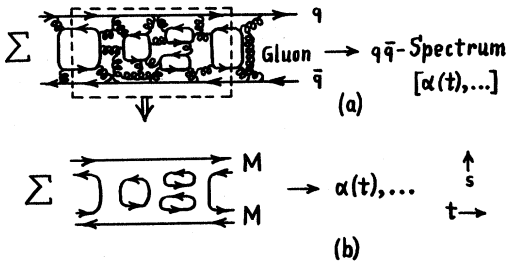

FIG. 1. Generation of hadronic $q\bar{q}$ spectrum taking into account quark loops.

In the DTU approach, one begins by simultaneously considering all the "ordered" planar fishnet graphs of Fig. 1(b).[2,4] These have the simplest topologies and can be argued to give a good first approximation to the hadron spectrum.[2,5] They have s-t channel crossing (where s and t are the usual Mandelstam variables), satisfy duality and exchange degeneracy exactly, and do not have the usual Regge cuts. This latter feature was not adequately taken into account in our previous approximate attempts to deal with Fig. 1(b) (Refs. 6–9) but is explicitly addressed in this paper, which goes beyond the calculations of Refs. 6–9 in other respects as well.

Once we have a solution of the above "planar-bootstrap" problem, physical amplitudes can be approximated by linear combinations of "ordered" amplitudes, and nonplanar effects can then be systematically brought in through a topological expansion. Earlier versions of DTU, while unambiguous and successful for $q\bar{q}$ mesons,[2] could not consistently take into account qqq and $qq\bar{q}\,\bar{q}$ states. Recently, however, Chew and Poenaru, and Stapp[5] have found a consistent way of overcoming this difficulty, without modifiying in any way the purely $q\bar{q}$ sector. In their scheme, one or more of the quark lines of Fig. 1(b) can be replaced by "diquarks" of a certain specified topological structure, and "Landau" lines, which are associated with the four-momenta of the hadrons in any given diagram, are introduced. It can be argued that the "interactions" of the latter lines with the diquarks must be weak. This means that diquark breakup and formation, and hence $qq\bar{q}\,\bar{q}\leftrightarrow q\bar{q}$ transitions, are forbidden in first approximation, so that $qq\bar{q}\,\bar{q}$ states should be narrow below the (qqq)-$(\bar{q}\,\bar{q}\,\bar{q})$ threshold.

At the lowest fully relativistic "zero-entropy" level of Ref. 5 where spin-momentum coupling is only dealt with approximately and the ordered amplitudes violate parity, it can be shown that the usual simple quark-model $q\bar{q}$ and qqq ground-state families are generated despite the presence of quark loops, and that an interesting "topological supersymmetry" property arises,[10] with realistic consequences for hadronic cross sections. In this paper, however, although we continue to assume the same quark-model families, we shall work at a more accurate planar ordered-amplitude level in which $qq\bar{q}\,\bar{q}\leftrightarrow q\bar{q}$ transitions remain suppressed, but in which parity is satisfied and the spin and momentum are properly coupled to each other.

In Sec. II we discuss the basic ingredients of our approach and in Sec. III we give a derivation, based on a simple dynamical approximation, of an explicit infinitely rising leading-Regge-trajectory formula for any given process. (A simplified physical picture of this is presented in Appendix A.) In Sec. IV we outline a general procedure for using this "generic" formula to calculate hadron masses, in which we require simultaneous consistency for entire sets of processes. In Sec. V we apply this to mesons in the exact flavor-SU(n) limit, e.g., to $q\bar{q}$ systems containing only u and d quarks; we find that our results are consistent with a simple metastable-string picture. In Sec. VI we turn to heavy mesons containing (u,d,c) and (u,d,b) quarks, for which certain additional assumptions have to be made. Finally, in Sec. VII we consider both light and heavy mesons containing s quarks by starting with uds degeneracy and then introducing a small K^*-ρ mass difference.

II. GENERAL DYNAMICAL CONSIDERATIONS

The set of graphs represented by Fig. 1(b) imply three properties which we will use in making our hadron-mass calculations.

A. Generalized ladder dynamics

For moderate t, Fig. 1(b) is approximately equivalent to the generalized infinite hadronic ladder sum of Fig. 2, which generates a leading "output" $q\bar{q}$ Regge trajectory, and in which the following hold.

(i) The masses of the vertical-line clusters $(a,\ldots)$, $(b,\ldots)$, $(c,\ldots)$ must be bounded to avoid double-counting, say, between Figs. 2(a) and 2(b).

(ii) The ladder exchanges in Fig. 2(b), 2(c),... themselves have the form of the entire sum of Fig. 2. In previous derivations of formulas for $\alpha(t)$ these were simply approximated by Regge exchanges.[6–9] We will not have to make this approximation in what follows.

Figure 2 will be symbolically represented by

$$12(a)34\longrightarrow\alpha \tag{2.1}$$

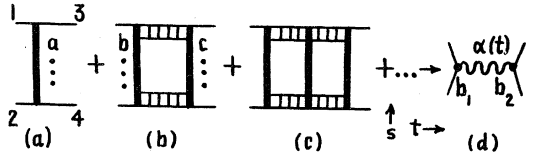

FIG. 2. Dominant contribution to Fig. 1(b) for moderate t.

if 1 and 2 are particles and by

$$\alpha_1\alpha_2(a)34\rightarrow\alpha \tag{2.2}$$

if they are arbitrary members of the Regge-trajectory families α_1 and α_2, with spins $S_1=\alpha_1(m_1{}^2)$ and $S_2=\alpha_2(m_2{}^2)$, and masses m_1 and m_2. There is no loss of generality in defining our initial state so that

$$S_1+S_2\geq S_3+S_4\ . \tag{2.3}$$

B. Duality

Figure 1(b) does not give the usual Regge cuts.[11] When combined with analyticity, it therefore implies simple finite-energy sum rule (FESR) duality, which can be used to relate Figs. 2(a) and 2(d) and gives (see, e.g., Appendix D)

$$\int_0^{\bar{s}} ds[\Gamma(t)\delta(s-s_a)-b_1(t)b_2(t)\nu^{\alpha(t)}\theta(\nu)] \times\nu^{-(S_1+S_2)}=0\ , \tag{2.4}$$

where the δ-function term is an approximation to the lowest nonvanishing contribution (of effective mass $\sqrt{s_a}$) to the s-channel absorptive part of Fig. 2(a), the constant $\bar{s}$ corresponds to a point approximately halfway between a and the next significant contribution above it (at least if we expect semi-local duality), and ν is the usual crossing-symmetric variable $\frac{1}{2}(s-u)$, which can also be written as

$$\nu=s+\tfrac{1}{2}\left[t-\sum_{i=1}^{4} m_i{}^2\right]\ . \tag{2.5}$$

We have taken the usual s-kinematic-singularity-free highest-helicity amplitude,[11] multiplied by a factor of ν^N, with the integer N adjusted so that the absorptive part of the resulting amplitude T has the asymptotic Regge behavior $b_1b_2\nu^\alpha$.

When $m_1=m_2$ or $m_3=m_4$, ν is proportional to the cosine of the c.m. scattering angle θ_t in the t channel and is thus the appropriate variable for Regge exchange. When $m_1\neq m_2$ and $m_3\neq m_4$ we have, instead,

$$\nu+\tfrac{1}{2}(m_1{}^2-m_2{}^2)(m_3{}^2-m_4{}^2)t^{-1}=2q_iq_f\cos\theta_t\ , \tag{2.6}$$

where q_i and q_f are initial and final t-channel c.m. three-momenta. Here a single Regge term proportional to $(\cos\theta_t)^\alpha$ or $P_\alpha(\cos\theta_t)$ will have a singularity at $t=0$ which is not present in the full amplitude,[11] and must be canceled by an infinite set of Regge daughters. A simple way of guaranteeing this is to take ν as our basic variable and to use a Regge term proportional to ν^α; this does not give any difficulties at $t=0$ but reduces exactly to a $(\cos\theta_t)^\alpha$ behavior when $m_1=m_2$ or $m_3=m_4$.

If we consider lower-helicity amplitudes or higher-moment sum rules, we must make the replacement

$$(S_1+S_2)\rightarrow S_1+S_2-n,\quad n=\text{ integer}>0\ . \tag{2.7}$$

Otherwise, everything remains the same as before.

C. Output-α uniqueness

The infinite set of sums of hadronic fishnet graphs represented by Fig. 1(b) is equivalent to a multichannel multiparticle generalization of a Bethe-Salpeter equation, which is itself a relativistic version of a Lippmann-Schwinger or Schrödinger equation. We would therefore expect a unique solution for the output $\alpha(t)$ and will assume that this is in fact the case in what follows.

III. EXPLICIT REGGE-TRAJECTORY FORMULA

We will now use the properties of Sec. II to derive an explicit infinitely rising leading-Regge-trajectory formula for any given process. Similar (but not identical) formulas were derived in special cases in Refs. 6–9. Some of the assumptions we will use here will be very different, however.

A. Representation for the Regge-trajectory function

To deal with Fig. 2, we will make an appropriate projection of the highest-helicity amplitude T introduced in Sec. II B. Now the projection which is associated with a partial diagonalization of t-channel unitary for $t>0$, and does not lead to any t-threshold singularities, is the modified Froissart-Gribov "partial-wave" projection[11]

$$T_j(t)=(2q_fq_i)^{-j-1}\int_0^\infty ds\,A(s,t)\hat{Q}_j(\cos\theta_j)\ , \tag{3.1}$$

where $A(s,t)$ is the s-channel absorptive part of T, normalized so $A=\mathrm{Im}T$ for $t<0$, and $\hat{Q}_j$ is a function related to a second-type Jacobi function (or a second-type Legendre function in the case of spinless-particle scattering). If we now expand $z^{j+1}\hat{Q}_j(z)$ in powers of z^{-2}, which decrease quite

rapidly for $|z|>1$, and then expand in powers of $1/t$, we obtain

$$\hat{T}_j(t)=\sum_{k=0}^{\infty}\sum_{h=0}^{\infty}c_{kh}(j)\left[\frac{(m_1{}^2-m_2{}^2)(m_3{}^2-m_4{}^2)}{2t}\right]^k \times(q_fq_i)^{2h}A_{j+k+2h}(t)\ , \tag{3.2}$$

where A_j is the Mellin transform

$$A_j(t)=\int_0^{\infty}d\nu A(s,t)\nu^{-j-1}\ . \tag{3.3}$$

In most cases we can approximate $\hat{T}_j$ by the $k=h=0$ term in the double sum of Eq. (3.3). When $m_1\neq m_2$ or $m_3\neq m_4$, however, q_fq_i is infinite and the higher terms in Eq. (3.2) can have infinite coefficients at $t=0$. This difficulty is related to the need for $j=\alpha-1$, $\alpha-2,\ldots$ daughter poles at $t=0$ for such processes[11] and can be circumvented, at least for the purposes of this paper, by simply using $A_j(t)$ instead of $\hat{T}_j(t)$ as our basic projection formula.

If we formally associate a coupling-strength parameter ϕ with each of the clusters $(a,\ldots)$, $(b,\ldots)$, $(c,\ldots)$, ..., the projected sum of Fig. 2 takes on the form of an expansion in ϕ

$$A_j(t)=\phi a_{1j}(t)+\phi^2a_{2j}(t)+\phi^3a_{3j}(t)+\cdots\ , \tag{3.4}$$

where ϕa_{1j} is the Mellin transform of Fig. 2(a), which gives, approximately,

$$\phi a_1(s,t)=\Gamma(t)\delta(s-s_a)+b_1(t)b_2(t)\nu^{\alpha(t)}\theta(s-\bar{s})\theta(s_0-s)\ . \tag{3.5}$$

The δ-function term is again an approximate to the lowest nonvanishing contribution in Fig. 2(a) and the Regge term takes into account all the higher $(s>\bar{s})$ contributions in the average-duality sense of Eq. (2.4). Since we are insisting on no double-counting between Figs. 2(a) and 2(b), we have inserted a step function $\theta(s_0-s)$ to exclude states above the effective threshold $s=s_0$ of Fig. 2(b). If we take the Mellin transform (3.3) of Eq. (3.5) we obtain

$$\phi a_{1j}(t)=\Gamma(t)\nu_a{}^{-j-1}+\frac{b_1(t)b_2(t)}{\alpha(t)-j}(\nu_0{}^{\alpha-j}-\bar{\nu}^{\alpha-j})\ , \tag{3.6}$$

where ν_a, ν_0, and $\bar{\nu}$ are given by Eq. (2.5), with $s=s_a$, s_0, and $\bar{s}$, respectively.

The δ functions of Eqs. (2.4) and (3.5) have particularly simple interpretations if $\sqrt{s_a}$ corresponds to a single particle. In practice, however, we might also have contributions from backgrounds, as well as from other particles, e.g., ones lying on possible daughter trajectories. Since single-particle states are generally still expected to provide the most important contributions, however, we continue to expect an expression of the form (3.5) to best approximate the absorptive part at low s, even though $\sqrt{s_a}$ may then be effectively shifted away from the mass of the lowest single-particle contribution.

If we take the $[1,N]$ Padé approximant of Eq. (3.4) we obtain, for a given t,

$$A_j=\frac{\phi a_{1j}}{1-K(j)}\ , \tag{3.7}$$

where

$$K(j)=\phi\frac{a_{2j}}{a_{1j}}+\phi^2\left[\frac{a_{3j}}{a_{1j}}-\left[\frac{a_{2j}}{a_{1j}}\right]^2\right]+\cdots \tag{3.8}$$

has N terms adjusted so that an expansion of Eq. (3.7) in powers of ϕ reproduces the first $(N+1)$ terms in Eq. (3.4). Now in the case of the lowest elastic process for a given set of quantum numbers, Eq. (3.7) satisfies elastic t-channel unitarity exactly for any finite value of N (see Appendix E). We thus expect the series (3.8) to converge fairly rapidly when we take $N\to\infty$. This is in fact trivially the case for factorizable models with $a_{nj}=u_jk_j{}^{n-1}v_j$, which are usually reasonable approximations to the graphs of Fig. 2 because of average duality between vertical-line clusters like $(b\cdots)$ and factorizable t-channel Regge behavior,[6] and which give $[1,N]=[1,1]$ for any N (see also Appendix A). If we use Eq. (3.3) we find, order by order, that Eq. (3.8) has the representation

$$K(j)=\int_{y_0}^{\infty}dy\,G(y)y^{-j-1}\ , \tag{3.9}$$

where $y_0=\nu_0/\nu_a$ (see Appendix F). With $N=1$ and $s_0=\bar{s}$, for example, we would have Eq. (3.9) with

$$G(\nu/\nu_a)=\nu_a\phi^2a_2(s,t)/\Gamma(t)\ .$$

From Eq. (3.7), A_j has a Regge pole at $j=\alpha$ if

$$K(\alpha)=1\ . \tag{3.10}$$

The corresponding residue, normalized as in Eqs. (2.4) and (3.5), is

$$b_1 b_2 = -\phi a_{1\alpha}/K'(\alpha) \ . \tag{3.11}$$

If we combine Eqs. (3.6), (3.10), and (3.11), we obtain

$$\frac{\Gamma}{b_1 b_2} \nu_a{}^{-\alpha-1} + \ln\left[\frac{\nu_0}{\bar{\nu}}\right] = -\frac{K'(\alpha)}{K(\alpha)} \ , \tag{3.12}$$

which, together with Eq. (3.9) and the FESR (2.4), gives

$$\frac{1}{\alpha+1-S_1-S_2}\left[\frac{\bar{\nu}}{\nu_a}\right]^{\alpha+1-S_1-S_2} + \ln\left[\frac{\nu_0}{\bar{\nu}}\right] = \frac{\int_{y_0}^{\infty} dy\, G(y) y^{-\alpha-1} \ln y}{\int_{y_0}^{\infty} dy\, G(y) y^{-\alpha-1}} \ . \tag{3.13}$$

The idea of combining ladder dynamics with FESR duality was first proposed in Ref. 12, and has seen many other applications since then.[1,4]

B. A peak approximation

The dynamics of our problem is now contained entirely within the function $G(y)$. In our previous treatments in Refs. 7–9 we assumed that the ladder exchanges of Figs. 2(b), 2(c) , ... could be replaced by Regge exchanges and that only the heavy vertical lines need be retained as intermediate states in using s-channel unitarity to evaluate the absorptive part; this leads to the usual two-Reggeon behavior $G(y) \propto y^{\alpha_{\text{cut}}}$ for large y, modulo logarithmic factors. In the case of Fig. 2(b), for example, it corresponds to retaining only the intermediate state cut by line I of Fig. 3(a). On the other hand, it is known that, by including higher intermediate states, such as the one cut by line II in Fig. 3(b), the $y^{\alpha_{\text{cut}}}$ behavior is canceled for large y, leading to a sharp falloff in y.[11] We therefore expect the peaked structure of Fig. 4, where we have also indicated the threshold effect of the successive opening up of the various s-channel intermediate-state channels associated with Figs. 2(b), 2(c),.... Such a peaking of $G(y)$ permits us, in turn, to make the approximation

$$\ln y \simeq \ln(\nu_1/\nu_a) \tag{3.14}$$

within the integral of Eq. (3.13), with an α-independent ν_1. In Appendix C we shall see that finite-width corrections to Eq. (3.14) should have a relatively small effect on our final expression for $\alpha(t)$.

Equations (3.13) and (3.14) reduce to the equation

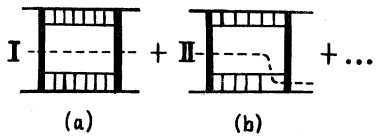

FIG. 3. Different intermediate-state contributions to Fig. 2(b), represented by the sets of lines cut by the dashed lines I, II,... .

$$e^X = c_1 X \ , \tag{3.15}$$

where

$$X = (\alpha+1-S_1-S_2)\ln(\bar{\nu}/\nu_a) \tag{3.16}$$

and

$$c_1 = 1 + \frac{\ln(\nu_1/\nu_0)}{\ln(\bar{\nu}/\nu_a)} \ . \tag{3.17}$$

Since c_1 is independent of α, and hence of X, Eq. (3.15) will, in general, have up to two solutions for X, and hence for α (case II in Fig. 5). In Sec. II C, however, we argued that the output α should be unique. If we impose this requirement, $Y = c_1 X$ must be tangent to $Y = e^X$ (case I in Fig. 5). This gives

$$c_1 = e, \quad X = 1 \ , \tag{3.18}$$

or, using Eqs. (3.16) and (3.17),

$$\nu_1 = \nu_0 (\bar{\nu}/\nu_a)^{e-1} \ , \tag{3.19}$$

$$\alpha(t) = S_1 + S_2 - 1 + \left[\ln\left[1 + \frac{\bar{s} - s_a}{\nu_a}\right]\right]^{-1} \ . \tag{3.20}$$

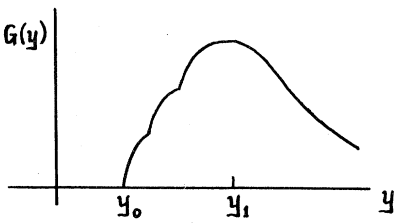

FIG. 4. Schematic plot of $G(y)$. The slope discontinuities arise because of the threshold effect of the successive opening up of the various s-channel intermediate-state channels associated with Fig. 2(b), 2(c),. ... .

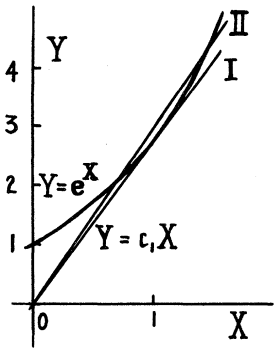

FIG. 5. Possible solutions of Eq. (3.15), arising from the intersection of $Y=e^X$ and $Y=c_1X$, with I corresponding to $c_1=e$ and II to $c_1>e$.

Equation (3.20) has branch points at $\nu_a=0$ and $\nu_a=-(\bar{s}-s_a)$, which can be joined by a cut in the ν_a plane. In Appendix G we argue that this singularity structure is spurious and that the approximation (3.14), and hence Eq. (3.20), are invalid in that region. In its valid nonsingular regions, however, Eq. (3.20) can be well approximated by

$$\alpha(t)=S_1+S_2+c+2\hat{\alpha}'\nu_a\ , \tag{3.21}$$

a form which exactly reproduces the $t\to\infty$ Eq. (3.20) limits of $\alpha'(t)$ and $[\alpha(t)-t\alpha'(\infty)]$ if we take

$$c=-\tfrac{1}{2},\quad 2\hat{\alpha}'=1/(\bar{s}-s_a)\ . \tag{3.22}$$

Since the approximation (3.22) then rapidly gets better and better as we go further away from the $-(\bar{s}-s_a)\lesssim\nu_a<0$ region of invalidity of Eq. (3.20) (see Fig. 6), we clearly can use either Eq. (3.20) or (3.21) for $\nu_a\lesssim-(\bar{s}-s_a)$ and $\nu_a\gtrsim 0$.

Equation (3.22) gives

$$\bar{s}=s_a+\tfrac{1}{2}\hat{\alpha}'^{-1}\ . \tag{3.23}$$

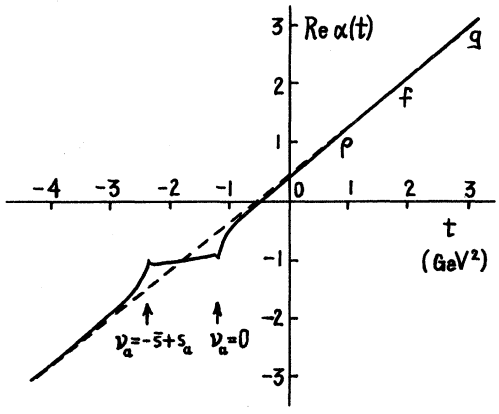

FIG. 6. Plots of Eqs. (3.20) (solid line) and (3.24) (dashed line) using Eqs. (3.23), (5.12), (5.13), and (5.14) for the process (5.1) ($\pi\pi$ scattering).

For processes in which the s- and t-channel Regge slopes are equal, this is consistent with the usual semilocal duality statement that $\bar{s}$ be at a point halfway between a and its first Regge recurrence, since $\hat{\alpha}'=\alpha'(t)$ from Eq. (3.21). This would be trivially the case for crossing-symmetric processes, for example, in which a lies on $\alpha(t)$.

Using Eqs. (2.5) and (3.22), Eq. (3.21) can also be written as

$$\alpha(t)\simeq S_1+S_2-\tfrac{1}{2}+2\hat{\alpha}'\left[s_a+\tfrac{1}{2}\left[t-\sum_{i=1}^{4}m_i^2\right]\right]\ . \tag{3.24}$$

IV. INTERPROCESS CONSISTENCY

The results (3.20) or (4.24) apply to a given specific process. The same output α can, however, arise for an infinite set of other processes. For example, we should have the same output $\alpha_\rho(t)$ both in $\rho\rho\to\rho\rho$ and in $\rho^r\rho^r\to\rho\rho$, where ρ^r is any Regge recurrence of ρ. Now the regions of invalidity $-(\bar{s}-s_a)\lesssim\nu_a\lesssim 0$ are different for these two processes, and we can use either Eq. (3.20) or Eq. (3.24) for $\nu_a\lesssim-(\bar{s}-s_a)$ and $\nu_a\gtrsim 0$, as we have seen. On the other hand, we can readily obtain *exactly* the same $\alpha(t)$ in the overlapping regions of validity for both processes if we use Eq. (3.24). Since Eq. (3.24) is linear in t, this also means that it continues to apply in a region $-(\bar{s}-s_a)\lesssim\nu_a\lesssim 0$ for one of these processes, provided this region corresponds to a range of t which is in a region of validity $\nu_a\lesssim-(\bar{s}-s_a),\nu_a\gtrsim 0$ for the other process. We shall see below that it is always possible to have such pairs of processes in which the regions of invalidity do not overlap, making it possible to apply Eq. (3.24) for any t. The same arguments do not apply to Eq. (3.20) and so we shall use Eq. (3.24) in what follows.

In making actual hadronic-mass calculations we simultaneously apply Eq. (3.24) to entire sets of processes and require consistency. For the class of output $\alpha(t)$ of a given quark content $(u\bar{u},\ldots s\bar{s},c\bar{u},\ldots c\bar{c},b\bar{u},\ldots b\bar{b},\ldots)$ we first order sets of hadronic processes according to increasing quark-mass content within the vertical line $(a,\ldots)$ of Fig. 2(a); this corresponds to decreasing dynamical importance of the corresponding external-horizontal-line channels (12,34) of Fig. 2, since these are then made up of particles having larger quark-mass content and lying on lower Regge trajectories. Within each such set we then require the following.

(i) Allowed couplings vanish, exactly or approximately, only if they are required to by consistency.

(ii) Possible secondary contributions to a in Fig. 2(a) (backgrounds or other states), whose net effect, as we saw in Sec. III A, would be to shift the effective value of $\sqrt{s_a}$ away from the mass m_{aL} of the lowest contributing single-particle state, are as small as possible. In other words, we assume that a is dominated by single-particle states unless consistency with other processes requires, say, a partial suppression of such states and a relative enhancement of the role of backgrounds. Higher states are , of course, explicitly excluded from a by the no-double-counting requirement and Eq. (3.23) when α' is the same in both s and t channels—unless, again, consistency requires at least a partial suppression of the lowest state.

The net effect of (i) and (ii) would be to require a simultaneous minimization of $|s_a - m_{aL}{}^2|$ for all the processes in a given set, with m_{aL} as low as possible. This would then be repeated for each set until all the possible parameters of our output-$\alpha(t)$ class have been extracted. We have no *a priori* guarantee, of course, that all of these parameters can be determined by our procedure, nor that the resulting solution is unique. In the case of the light-quark $q\bar{q}$ systems containing u,d,s quarks, however, this does turn out in fact to be the case, given only the ρ and K^* masses, one of which merely serves to set the energy scale.

In the rest of this paper we shall only be concerned with $M=q\bar{q}$ mesons. It then turns out to be sufficient to consider processes of the type

$$MM(M)MM \to \alpha_M \ , \tag{4.1}$$

which are expected to be dynamically the most important for ouput α_M.

V. APPLICATION TO $q\bar{q}$ MESONS IN THE EXACT FLAVOR-SU (n) LIMIT

Here the ground states are the vector $\hat{\rho}$ and the pseudoscalar $\hat{\pi}$. If $n=2$, for example, $\hat{\rho}=(\rho,\omega)$ and $\hat{\pi}=(\pi,\eta_{ud})$, where each pair is mass-degenerate at our planar level. Now, in order to carry out the $|s_a - m_{aL}{}^2|$-minimization procedure of Sec. IV, it is sufficient to consider only $\hat{\rho}$ and $\hat{\pi}$ for the particles 3 and 4 in Fig. 1, since their Regge recurrences would automatically require higher s_a for the same $\alpha(t)$ in Eq. (3.24).

Parity requires the mass of the lowest allowed single state to be $m_{aL}=m_{\hat{\rho}}$ for the processes

$$\alpha_{\hat{\pi}}\alpha_{\hat{\pi}}(a)\hat{\pi}\hat{\pi} \to \alpha_{\hat{\rho}} \ , \tag{5.1}$$

$$\alpha_{\hat{\pi}}\alpha_{\hat{\rho}}(a)\hat{\pi}\hat{\pi} \to \alpha_{\hat{\rho}} \ , \tag{5.2}$$

$$\alpha_{\hat{\rho}}\alpha_{\hat{\pi}}(a)\hat{\rho}\hat{\pi} \to \alpha_{\hat{\pi}} \ , \tag{5.3}$$

$$\alpha_{\hat{\pi}}\alpha_{\hat{\rho}}(a)\hat{\pi}\hat{\rho} \to \alpha_{\hat{\rho}} \ . \tag{5.4}$$

In this case we can have $s_a \le m_{aL}{}^2$ if $m_{\hat{\rho}} > 2m_{\hat{\pi}}$. The remaining parity-allowed processes, for which $m_{aL}=\min(m_{\hat{\pi}},m_{\hat{\rho}})$, are

$$\alpha_{\hat{\rho}}\alpha_{\hat{\rho}}(a)\hat{\pi}\hat{\pi} \to \alpha_{\hat{\rho}} \ , \tag{5.5}$$

$$\alpha_{\hat{\rho}}\alpha_{\hat{\rho}}(a)\hat{\pi}\hat{\rho} \to \alpha_{\hat{\pi}} \ , \tag{5.6}$$

$$\alpha_{\hat{\rho}}\alpha_{\hat{\rho}}(a)\hat{\rho}\hat{\rho} \to \alpha_{\hat{\pi}} \ , \tag{5.7}$$

$$\alpha_{\hat{\rho}}\alpha_{\hat{\pi}}(a)\hat{\pi}\hat{\rho} \to \alpha_{\hat{\pi}} \ , \tag{5.8}$$

$$\alpha_{\hat{\rho}}\alpha_{\hat{\rho}}(a)\hat{\pi}\hat{\rho} \to \alpha_{\hat{\rho}} \ , \tag{5.9}$$

$$\alpha_{\hat{\pi}}\alpha_{\hat{\rho}}(a)\hat{\rho}\hat{\pi} \to \alpha_{\hat{\rho}} \ , \tag{5.10}$$

$$\alpha_{\hat{\rho}}\alpha_{\hat{\rho}}(a)\hat{\rho}\hat{\rho} \to \alpha_{\hat{\rho}} \ , \tag{5.11}$$

Here we must have $s_a \ge m_{aL}{}^2$. One can readily show that, given α' to fix our energy scale, a simultaneous minimization of the $|s_a - m_{aL}{}^2|$, subject to the above constraints, gives, using Eqs. (3.24),

$$\alpha'(s_a - m_{aL}{}^2) = 0, -\tfrac{1}{4}, -\tfrac{1}{4}, 0, 0, 0, \tfrac{1}{4}, \tfrac{1}{4}, \tfrac{1}{4}, \tfrac{1}{2}, \tfrac{1}{2} \tag{5.12}$$

for Eqs. (5.1)–(5.11). For example, a decrease of s_a for Eq. (5.10) leads immediately to $s_a < m_\pi{}^2$ for Eq. (5.5), whereas a decrease of s_a for Eq. (5.11) leads to $s_a < m_\pi{}^2$ for Eq. (5.6). Thus Eq. (5.12) does correspond to a constrained minimization of $\max|s_a - m_{aL}{}^2|$ for Eqs. (5.1)–(5.11). It also corresponds to a similar minimization for various subsets of Eqs. (5.1)–(5.11).

The solution (5.12) leads to the results

$$\alpha'_{\hat{\pi}} = \alpha'_{\hat{\rho}} = (2m_{\hat{\rho}}{}^2)^{-1} \tag{5.13}$$

and

$$m_{\hat{\pi}}{}^2 \simeq m_{\hat{\rho}}{}^2 - (2\alpha'_{\hat{\rho}})^{-1} = 0 \ , \tag{5.14}$$

which gives $\alpha_{\hat{\rho}}(0)=0.5$ and $\alpha_{\hat{\pi}}(0)=0$; if we take $m_\rho = 0.776$ GeV, we obtain $\alpha'_{\hat{\rho}} = 0.833$ GeV^{-2}, in good agreement with experiment.

If we replace the particles 3 and 4 for any one of the equations (5.1)–(5.11) by their Nth and Mth Regge recurrences, we must make the replacement $s_a \to s_a + \frac{1}{2}(N+M)\alpha'^{-1}$ in Eq. (3.24) (see Fig. 2). Similar increases in s_a also occur if we use higher-moment versions of the finite-energy sum rule

(2.4), or lower-helicity amplitudes, in which case we must make the replacement (2.7). Such increases of s_a do not violate any of our constraints and would arise, for example, if we have a decoupling of one or more of the lowest states contributing to the vertical line of Fig. 2(a); this sort of decoupling is similar to the introduction of nonsense wrong-signature zeros in standard Regge theory[11] and is known to arise quite naturally in multichannel dynamics, e.g., in nuclear physics.

Our present model is strictly planar, with mass-degenerate $\hat{\pi}=(\pi,\eta_{ud})$ for $n=2$, so that there is, in some sense, no distinction between π and $\eta_{ud}=(u\bar{u}+d\bar{d})/\sqrt{2}$. This should be contrasted with the results of Ref. 6, where we imposed G parity on our amplitudes, which were, nevertheless, assumed to be at least approximately planar (exact planarity is inconsistent with G parity for "ordered" amplitudes[13]). This is a crude way of introducing higher-order "cylinder" corrections[2] and leads to a breaking of π-η_{ud} degeneracy.[14] The α_π, α_ρ, and α_ω trajectories turn out to be the same as in the exact planar case, however.

It is interesting to note that, as long as the widths of the particles on the leading Regge trajectory $\alpha(t)$ remain relatively narrow, the above linear-trajectory light-quark system results are consistent, for moderate and high α, with a metastable-string picture[9] in which Fig. 1 corresponds to a rotating string[13,15] or narrow tube of hadronic matter; this matter is not stable, but condenses into a line of hadrons (through light $q\bar{q}$ creation) which stick together for a while and then break up (see Fig. 7 and Refs. 9 and 16). As long as its lifetime is long enough, however, we still have, in the classical limit, the leading-trajectory $\alpha(t)=L(t)-S_1-S_2$ result:

$$L(t)\simeq t(2\pi T_0)^{-1} \quad \text{for large } t \tag{5.15}$$

$$\simeq \frac{1}{T_0}\left[\frac{m_1 m_2}{m_1+m_2}\right]^{1/2}(\sqrt{t}-m_1-m_2)$$

$$\text{for } t\sim(m_1+m_2)^2, \tag{5.16}$$

where m_1,m_2 are the masses and S_1,S_2 the spins of the particles 1,2 at the ends of the string; we have taken an approximately constant string tension T_0 in order to reproduce the linear form (3.24) for large t. The classical limit breaks down, of course, for the ground state but should be reasonable for all excited states. In this region T_0 should also be universal, since $\alpha'_{\hat{\pi}}=\alpha'_{\hat{\rho}}$. This is consistent with the notion that T_0 only depends on the matter in the hadronic tube between the end particles 1 and 2 and not on 1 and 2 themselves.

FIG. 7. Hadron condensation along a metastable rotating "string" joining a valence $q_v\bar{q}_v$ pair.

VI. APPLICATION TO u,d,c AND u,d,b MESONS

In principle, the results of Sec. V already give a solution for mesons containing u,d,c,b quarks, in which we have mass-degenerate $(\rho,\omega,D^*,\psi,B^*,\Upsilon)$ and $(\pi,\eta_{ud},D,\eta_c,B,\eta_b)$ states, where $(D^*,D)=(c\bar{u},c\bar{d})$, $(\psi,\eta_c)=c\bar{c}$, $(B^*,B)=(b\bar{u},b\bar{d})$, and $(\Upsilon,\eta_b)=b\bar{b}$. However, if we insist on a large *a priori* mass difference between, say, ρ and ψ, we find that another solution is in fact possible, at least if we restrict ourselves to the lowest heavy-meson states, provided we allow a systematic decoupling of the lowest light-meson states from the vertical-line clusters $a,\ldots$ in Fig. 2(a). Except for a minimal number of extra decouplings needed to achieve this, however, we will continue to impose our rules (i) and (ii) of Sec. IV, and, in particular, a minimization of background contributions to a.

A. Mesons containing u,d,c quarks

The dominant lowest-s_a processes giving output $c\bar{c}$ Regge trajectories and corresponding to Eqs. (5.1)–(5.11) are

$$\alpha_D\alpha_D(a_1)DD\to\alpha_\psi\,, \tag{6.1}$$

$$\alpha_D\alpha_{D^*}(a_2)DD\to\alpha_\psi\,, \tag{6.2}$$

$$\alpha_{D^*}\alpha_D(a_3)D^*D\to\alpha_{\eta_c}\,, \tag{6.3}$$

$$\alpha_D\alpha_{D^*}(a_4)DD^*\to\alpha_\psi\,, \tag{6.4}$$

with $m_a=m_{\hat{\rho}}$ and

$$\alpha_{D^*}\alpha_{D^*}(a_5)DD\to\alpha_\psi\,, \tag{6.5}$$

$$\alpha_{D^*}\alpha_{D^*}(a_6)DD^*\to\alpha_{\eta_c}\,, \tag{6.6}$$

$$\alpha_{D^*}\alpha_{D^*}(a_7)D^*D^*\to\alpha_{\eta_c}\,, \tag{6.7}$$

$$\alpha_{D^*}\alpha_D(a_8)DD^*\to\alpha_{\eta_c}\,, \tag{6.8}$$

$$\alpha_{D^*}\alpha_{D^*}(a_9)DD^*\to\alpha_\psi\,, \tag{6.9}$$

$$\alpha_D\alpha_{D^*}(a_{10})D^*D\to\alpha_\psi\,, \tag{6.10}$$

$$\alpha_{D^*}\alpha_{D^*}(a_{11})D^*D^*\to\alpha_\psi\,, \tag{6.11}$$

with $m_{aL}=m_\pi{}^2$ and $s_a \geq m_{aL}{}^2$.

In Sec. V, we had a situation where the s- and t-channel Regge slopes α' were equal, so that Eqs. (3.23) and (3.24) gave the semilocal duality result that $\bar{s}$ be halfway between a and the Regge recurrence immediately above it. This need not the case for Eqs. (6.1)–(6.11), where we have heavy $q\bar{q}$ states in the t channel and light $q\bar{q}$ states in the s channel. If, moreover, we apply the metastable string picture of Fig. 7 to π, D, η_c,..., and ρ, D^*, ψ,..., we find that, since $m_\psi \gg m_\rho$, we must have, for low α,

$$\alpha'_{\hat{\rho}} > \alpha'_{D^*} \simeq \alpha'_D > \alpha'_\psi \simeq \alpha'_{\eta_c} . \tag{6.12}$$

In particular, this follows immediately from Eqs. (5.15) and (5.16), where T_0 is, as we have seen, universal. It continues to be true under much more general conditions, however, as long as we remember that the material in the hadronic tube between 1 and 2 is independent of the flavor of the end particles 1 and 2 themselves.

If we assume that $\bar{s}$, and hence α', continues to be approximately constant in the region of the lowest states where Eq. (6.12) applies, we find, on applying Eqs. (3.24) and (3.22), that consistency among the processes (6.1)–(6.11) leads to

$$s_{a_i} = m_{aL}{}^2 + \tfrac{1}{2}\epsilon_i \alpha'^{-1}_{\hat{\rho}} - \tfrac{1}{2}(\alpha_1+\alpha_2-\alpha_1^0-\alpha_2^0)(\alpha'^{-1}_\psi - \alpha'^{-1}_{D^*}) \tag{6.13}$$

with $\alpha'_\psi = \alpha'_{\eta_c}$ and $\alpha'_{D^*} = \alpha'_D$, which must be strict equalities if we are to maximize the number of cases where $\sqrt{s_{a_i}}$ corresponds to the mass of a single state. Here α_i^0 is the lowest spin of any particle on the trajectory α_i for the general process (2.2) and

$$\epsilon_1 = 3N-3\delta-\gamma-1+\epsilon_6 , \tag{6.14}$$

$$\epsilon_2 = 2N-2\delta-\gamma-1+\epsilon_6 , \tag{6.15}$$

$$\epsilon_3 = N-\delta-1+\epsilon_6 , \tag{6.16}$$

$$\epsilon_4 = 2N-\delta-\gamma-1+\epsilon_6 , \tag{6.17}$$

$$\epsilon_5 = N-\delta-\gamma+\epsilon_6 , \tag{6.18}$$

$$\epsilon_7 = \delta+\epsilon_6 , \tag{6.19}$$

$$\epsilon_8 = N-\delta+\epsilon_6 , \tag{6.20}$$

$$\epsilon_9 = N-\gamma+\epsilon_6 , \tag{6.21}$$

$$\epsilon_{10} = 2N-\delta-\gamma+\epsilon_6 , \tag{6.22}$$

$$\epsilon_{11} = N-\gamma+\delta+\epsilon_6 , \tag{6.23}$$

where N is given by

$$\alpha'_{\eta_c} = \alpha'^{-1}_\psi = N\alpha'^{-1}_{\hat{\rho}} \tag{6.24}$$

and

$$\delta = (m_{D^*}{}^2 - m_D{}^2)\alpha'^{-1}_{\hat{\rho}} , \tag{6.25}$$

$$\gamma = (m_\psi{}^2 - m_{\eta_c}{}^2)\alpha'^{-1}_{\hat{\rho}} . \tag{6.26}$$

If, furthermore, we replace the particles 3 and 4 of Eqs. (2.2) by any of their Regge recurrences, so that

$$\alpha_3^0 \to \alpha_3, \quad \alpha_4^0 \to \alpha_4 , \tag{6.27}$$

we must also make the replacement

$$s_{a_i} \to s_{a_i} + \tfrac{1}{2}(\alpha_3+\alpha_4-\alpha_3^0-\alpha_4^0)\alpha'^{-1}_{D^*} \tag{6.28}$$

in Eq. (6.13).

If we did not have the constraint (6.12), we can readily see that Eqs. (6.13)–(6.23) reduce to Eq. (5.12), which then corresponds to the solution with the lowest $|s_a - m_{aL}{}^2|$, and also gives Regge-slope universality. With the inequalities of (6.12), however, we see from Eq. (6.13) that s_{a_i} decreases with increasing α_1 and α_2. This is obviously absurd for large values of the latter quantities. We must remember, however, that Eq. (6.12) only applies for low α, that Eq. (3.24) itself can only be expected to hold for a limited range of $\sqrt{t}$, at least on the charmed-mass scale, and, finally, that the dominant channels for a given t must correspond to $2m_1 \approx 2m_2 \approx \sqrt{t}$. We shall therefore restrict ourselves to small values of α_1 and α_2.

If we assume that the inequalities (6.12) are associated with a minimal number of extra decouplings of lowest-state contributions to the a_i and if we insist on an overall minimization of secondary contributions to the a_i (see Sec. IV), Eqs. (6.13) and (6.28) would require integer N and n in Eq. (6.24) and in

$$\alpha'^{-1}_D = \alpha'^{-1}_{D^*} = n\alpha'^{-1}_{\hat{\rho}} . \tag{6.29}$$

This would guarantee, for example, that processes with no secondary contributions to a when $\alpha_i = \alpha_i^0$ will also essentially never have any secondary contribution when $\alpha_i \neq \alpha_i^0$. We must also require the ϵ_i to be as low as possible and to correspond to a maximization of the number of cases where $\sqrt{s_{a_i}}$ corresponds to the mass of a single-particle state.

Although other solutions are possible, the solution with the minimum nonzero breaking of D^*-D and ψ-η_c mass degeneracy (which we have at the

lowest-order "zero-entropy" level of Ref. 5) would then require, with all of our above constraints,

$$N=3,\quad n=2,\quad \delta=\gamma=\tfrac{1}{2},\quad \epsilon_6=0\ . \tag{6.30}$$

This corresponds to the smallest value of N, and hence of the ϵ_i, which is consistent with Eq. (6.12). If we now apply Eqs. (3.24), (6.13), (6.23), (6.24), (6.29), and (6.30) to, say, Eq. (6.11), we obtain

$$m_{D^*}{}^2=\tfrac{1}{4}m_\psi{}^2+\tfrac{1}{2}(m_\rho{}^2+\alpha'^{-1}_{\hat{\rho}}) +\tfrac{1}{8}\alpha'^{-1}_{\psi}\ . \tag{6.31}$$

Taking $m_\psi=3.10$ GeV, this gives $m_{D^*}=1.94$ GeV, which should be compared with the observed $D^*(2.01)$ mass. We also obtain, using Eq. (5.13),

$$m_{D^*}{}^2-m_D{}^2=m_\psi{}^2-m_{\eta_c}{}^2=\tfrac{1}{2}\alpha'^{-1}_{\hat{\rho}}\simeq m_\rho{}^2\ , \tag{6.32}$$

which is in good agreement with experiment. Finally, Eqs. (6.24) and (6.30) give a 2^+ $c\bar{c}$ Regge recurrence of mass 3.63 GeV, which can be identified with the familar $\chi(3.55)$ state.

In the above considerations we did not consider processes involving channels like πD^*, ρD, etc., with one charmed and one uncharmed meson, which give α_{D^*} and α_D as output. However, it turns out that in this case it is not possible to find a solution in which any of the s_a correspond to $s_a=m_{aL}{}^2$ for these processes, at least with $m_{D^*}{}^2(\gg m_\rho{}^2)$ close to the experimental value. Thus such processes will not help us in determining any parameters which are not already determined by the processes which give α_ψ and α_{η_c} as output.

B. Mesons containing u,d,b quarks

Our procedure and results here are very similar to the ones in (A). If we apply the metastable string picture of Fig. 7 to $\rho,B^*,\Upsilon,\ldots$ and $\pi,B,\eta_b,\ldots$ with $m_\Upsilon\gg m_\rho$, we obtain, for low α, the analog of Eq. (6.12):

$$\alpha'_{\hat{\rho}}>\alpha'_{B^*}\approx\alpha'_B>\alpha'_\Upsilon\approx\alpha'_{\eta_b}\ . \tag{6.33}$$

In addition, if $q_v=u,d$ in Fig. 8, the low-state dynamics of any $Q_v\bar{q}_v$ system with $Q_v=c$ is essentially the same as that of the corresponding system with $Q_v=b$, since in both cases we have the same light-quark-"string" rotating around a static heavy-quark center. We must therefore have

$$\alpha_{B^*}((m_{B^*}+m')^2)\simeq\alpha_{D^*}((m_{D^*}+m')^2) \tag{6.34}$$

with $m'\ll m_{D^*}$, so that

$$m_{B^*}\alpha'_{B^*}\simeq m_{D^*}\alpha'_{D^*}\ . \tag{6.35}$$

Similarly, we must also have

$$m_B\alpha'_B\simeq m_D\alpha'_D\ . \tag{6.36}$$

Except for a replacement of D, D^*, η_c, and ψ by B, B^*, η_b, and Υ, we again have Eqs. (6.1)–(6.29). Now if we are to prevent the possibility of s_a becoming negative when we increase all the α_i simultaneously by the same amount, we must have $n\geq N/2$. If, at the same time, we wish to minimize these high-α_i values of s_a, we must have $n=N/2$ if N is even and $n=(N+1)/2$ if N is odd, since n must be an integer, as we have seen. Now, for a given m_{B^*}, the value of n is essentially determined by Eq. (6.35) and $\alpha'^{-1}_{B^*}=n\alpha'^{-1}_{\rho}$, which is the b-quark equivalent of Eq. (6.29). This does not, by itself, enable us to determine whether we have the even value $2n$ or the odd value $(2n-1)$ for N. If, however, we take the solution with the minimum nonzero breaking of B^*-B and Υ-η_b mass degeneracy and the lowest possible values of the ϵ_i for that n, we must have

$$N=2n-1,\quad \delta=\gamma=\tfrac{1}{2}\ ,\qquad \epsilon_6=0\ ,\quad \alpha'_{B^*}=\alpha'_B\ . \tag{6.37}$$

If we then combine Eq. (3.24) with our modified Eqs. (6.13), (6.23), (6.29), (6.30), and (6.12) we obtain

$$m_{B^*}{}^2=\tfrac{1}{4}m_\Upsilon{}^2+\tfrac{1}{2}(m_\pi{}^2+\tfrac{1}{2}N\alpha'^{-1}_{\hat{\rho}})+\tfrac{1}{8}\alpha'^{-1}_{\Upsilon}\ . \tag{6.38}$$

If we now take $m_\Upsilon=9.46$ GeV, we can require N to be such that we have values of $\alpha'^{-1}_\Upsilon=N\alpha'^{-1}_{\hat{\rho}}$ and $\alpha'^{-1}_B=n\alpha'^{-1}_{\hat{\rho}}$ which satisfy Eq. (6.35) as closely as possible, using Eqs. (6.37) and (6.38), and the results $m_{D^*}=1.94$ GeV and $\alpha'^{-1}_{D^*}=2\alpha'^{-1}_{\hat{\rho}}$ obtained in the preceding subsection. This gives $n=5$, $m_{B^*}=5.14$ GeV, and $m_B=5.08$ GeV, a value slightly below the range $5.16<m_B<5.27$ GeV obtained experimentally at CESR.

It is interesting to note that our results give

$$m_\psi\alpha'_\psi\simeq m_\Upsilon\alpha'_\Upsilon,\quad m_{\eta_c}\alpha'_{\eta_c}\simeq m_{\eta_b}\alpha'_{\eta_b}\ , \tag{6.39}$$

which would also be obtained if we assumed an effective $\ln r$ potential between the $c\bar{c}$,$b\bar{b}$ valence

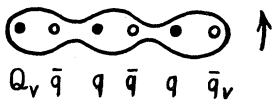

FIG. 8. Hadron condensation along a metastable rotating "string" joining $\bar{q}_v$ to a much heavier Q_v, which is then approximately static for lower energies.

quarks, or, alternatively, the corresponding end mesons in Fig. 7.

VII. APPLICATION TO MESONS CONTAINING s QUARKS

As in the case of systems containing u,d,c,b quarks, it is always possible to have a solution in which we do not have any mass change when we replace a u or d quark by an s quark. Unlike the c- or b-quark cases, however, this mass degeneracy is not broken very drastically in the real world and is therefore presumably associated with the presence of nonresonant backgrounds in the lowest contributions (a) of Fig. 2(a); it may even be associated with nonplanar corrections, as we shall see in Sec. VIII. In practice, we shall therefore begin with an exact-flavor-SU(3) solution and then study the consequences of introducing the minimum background needed to give a positive K^*-ρ mass difference.

A. Mesons containing u,d,s quarks

In the exact-flavor-SU(3) limit we simply have the results of Sec. V, where the values (5.12) of $|s_a-m_{aL}{}^2|$ were as low as possible. If we are to have $m_{K^*}>m_\rho$, however, we must take the list (5.1)–(5.11) for $q=u,d$ and expand it to include many additional processes involving $s\bar{s}$ and strange mesons. For example, in addition to Eq. (5.5), we must have the associated processes

$$\alpha_{K^*}\alpha_{K^*}(a)\hat{\pi}\hat{\pi}\to\alpha_{\hat{\rho}}\ , \tag{7.1}$$

$$\alpha_{\hat{\rho}}\alpha_{\hat{\rho}}(a)KK\to\alpha_{\hat{\rho}}\ , \tag{7.2}$$

with $m_{aL}=m_K$,

$$\alpha_{K^*}\alpha_{K^*}(a)KK\to\alpha_{\hat{\rho}}\ , \tag{7.3}$$

with $m_{aL}=m_{\eta_s}$,

$$\alpha_{K^*}\alpha_{\hat{\rho}}(a)K\hat{\pi}\to\alpha_{K^*},\ \text{etc.}, \tag{7.4}$$

with $m_{aL}=m_{\hat{\pi}}$, etc. Here additional background contributions must be brought in which would raise s_a above the value given by Eq. (5.12) for most of the processes involved. These contributions cannot be calculated *a priori* unless we have a more detailed model. However, in the cases where the output α does not contain s quarks, as in Eqs. (7.1)–(7.3), the minimum-background lowest $|s_a-m_{aL}{}^2|$ values of Eq. (5.12) can be consistently attained as before. We then recover the results of Sec. V for systems without s quarks and also obtain

$$m_\phi{}^2-m_{K^*}{}^2=m_{K^*}{}^2-m_{\hat{\rho}}{}^2 =m_K{}^2-m_{\hat{\pi}}{}^2=m_{\eta_s}{}^2-m_K{}^2\ , \tag{7.5}$$

$$\alpha'_{K^*}=\alpha'_\phi=\alpha'_K=\alpha'_{\eta_s}=\alpha'_{\hat{\rho}}\ . \tag{7.6}$$

The results (7.5) and (7.6) are in good agreement with experiment, except for m_{η_s}. We must remember, however, that both η_{ud} and η_s are expected to have important higher-order "cylinder" corrections, which are expected to shift their masses.[2,14]

B. $c\bar{s}$ mesons

In this case we can obtain all of our results from fairly general properties of the metastable string picture of Figs. 7 and 8, using Eq. (3.24) only to justify linear forms for the $c\bar{s}$ Regge trajectories. Now if we compare, say, α_{D^*} with the light-quark trajectory $\alpha_{\hat{\rho}}$, we see that, at least for excited states in their c.m. system, we expect

$$2\alpha_{D^*}((m_{D^*}+C+m/2)^2)=\alpha_{\hat{\rho}}(m^2)+K\ , \tag{7.7}$$

since the dynamics of a light-quark $q_v=(u,d)$ "string" of mass $m/2$ rotating about a static heavy-quark center $Q_v=c$ in Fig. 8 is essentially the same as that of half of the $q_v=(u,d)$, $\bar{q}_v=(\bar{u},\bar{d})$ string of Fig. 7 with mass m. If we next repeat this, but now with $q_v=s$ instead of $q_v=(u,d)$ everywhere, we obtain

$$2\alpha_{F^*}((m_{D^*}+C+m/2)^2)=\alpha_\phi(m^2)+K \tag{7.8}$$

with the same constants K and C. If we then combine Eqs. (7.7) and (7.8) and use the fact that $\alpha_\rho(t)$ and $\alpha_\phi(t)$ are parallel and linear in t, we obtain

$$2[\alpha_{D^*}(t)-\alpha_{F^*}(t)]=\alpha'_{\hat{\rho}}(m_\phi{}^2-m_{\hat{\rho}}{}^2)\ . \tag{7.9}$$

If, finally, we use Eq. (3.24) to justify linear forms for $\alpha_{D^*}(t)$ and $\alpha_{F^*}(t)$, at least in localized regions just above $m_{D^*}^2$ and $m_{F^*}^2$, we obtain

$$m_{F^*}^2-m_{D^*}^2=(m_{K^*}^2-m_{\hat{\rho}}^2)\alpha'_{\hat{\rho}}/\alpha'_{D^*},\quad \alpha'_{F^*}=\alpha'_{D^*}\ , \tag{7.10}$$

where we have also used Eq. (7.5). If we repeat the same procedure for the corresponding pseudoscalar trajectories, we obtain

$$m_F^2-m_D^2=(m_K^2-m_{\hat{\pi}}^2)\alpha'_{\hat{\pi}}/\alpha'_D,\quad \alpha'_F=\alpha'_D\ , \tag{7.11}$$

which, when combined with Eqs. (7.10), (6.29), and (5.13), also gives

$$m_{F^*}^2-m_F^2=m_{D^*}^2-m_D^2\ . \tag{7.12}$$

Although the F and F^* masses are not as well know as the D and D^* masses experimentally, these results, when combined with Eqs. (6.29), (6.30), and (5.13), are in agreement with present experimental data.

C. $b\bar{s}$ Mesons

The above considerations also apply with $Q_v=b$ instead of c in Fig. 8. If H^* and H are the vector and pseudoscalar $b\bar{s}$ states, we obtain

$$\begin{aligned} m_H^2-m_B^2&=m_{H^*}^2-m_{B^*}^2\\ &=(m_{K^*}^2-m_{\hat{\rho}}^2)\alpha'_{\hat{\rho}}/\alpha'_{B^*}\ , \end{aligned} \tag{7.13}$$

$$\alpha'_{H^*}=\alpha'_{B^*}=\alpha'_B=\alpha'_H\ . \tag{7.14}$$

If Eq. (7.13) is combined with Eqs. (7.10) and (7.11) we also have

$$\begin{aligned} m_H^2-m_B^2&=m_{H^*}^2-m_{B^*}^2\\ &=(m_{F^*}^2-m_{D^*}^2)\alpha'_{D^*}/\alpha'_{B^*}\ . \end{aligned} \tag{7.15}$$

Actually, Eq. (7.15) can also be obtained more directly, and in a less model-dependent way, by again noting, as in Sec. VI B, that if $q_v=s$ in Fig. 8, the low-state dynamics of any $Q_v\bar{q}$ system with $Q_v=c$ is essentially the same as that of the corresponding system with $Q_v=b$, since in both cases we have the same light-quark-"string" rotating around a static heavy-quark center. We must therefore have

$$\alpha_{H^*}((m_{B^*}+m')^2)=\alpha_{F^*}((m_{D^*}+m')^2) \tag{7.16}$$

with $m'\ll m_{D^*}$, so that

$$m_{B^*}\alpha'_{H^*}=m_{D^*}\alpha'_{F^*}\ . \tag{7.17}$$

Since $m_{B^*}-m_{H^*}\ll m_{H^*}$ and $m_{F^*}-m_{D^*}\ll m_{D^*}$, this also implies, when combined with Eqs. (6.35), that $\alpha'_{H^*}\simeq\alpha'_{B^*}$ and $\alpha'_{F^*}=\alpha'_{D^*}$. If, in addition, we combine Eqs. (6.34) and (7.16), and use Eq. (3.24) to justify linear forms for $\alpha_{D^*}(t)$, $\alpha_{F^*}(t)$, $\alpha_{B^*}(t)$, and $\alpha_{H^*}(t)$, at least in localized regions just above $m_{D^*}^2$, $m_{F^*}^2$, $m_{B^*}^2$, and $m_{H^*}^2$, respectively, we obtain

$$\alpha'_{B^*}(m_{H^*}^2-m_{B^*}^2)\simeq\alpha'_{D^*}(m_{F^*}^2-m_{D^*}^2)\ . \tag{7.18}$$

If we repeat this argument for pseudoscalar mesons and use Eqs. (6.29) and (6.37) to relate α'_D, α'_{D^*}, α'_B, and α'_{B^*}, we obtain Eq. (7.15) and the relations $\alpha'_H=\alpha'_B$ and $\alpha'_F=\alpha'_D$.

VIII. CONCLUSION

We have considered a scheme which, unlike many others, takes light-sea-quark loops into account, even in lowest order. We are then led, quite naturally, not only to infinitely rising Regge trajectories, but also to a small value of m_π^2/m_ρ^2, which has often been difficult to obtain in the past. We also obtain a constant α_ρ-α_π Regge-trajectory splitting, which, if it were to be described in terms of an effective $q\bar{q}$ potential, would require a long-range spin-spin interaction. Our only free parameters are the ρ, K^*, ψ, and Υ masses, one of which merely serves to fix the energy scale.

Our results were based on fairly general dynamical considerations and do not seem to depend on the details of any underlying model or theory. In this respect the situation is similar to the one for many other many-body problems, where one often gets almost the same results from widely different underlying Lagrangians. It may not be the case for couplings, however, which are discussed in Appendix B.

In this paper we restricted ourselves to $q\bar{q}$ mesons, although successful results have also been obtained (in collaboration with Nicolescu) for qqq and $qq\bar{q}\,\bar{q}$ systems, which will be presented in a separate paper. Our simplest and most natural solution, which also involves the fewest assumptions, is one for which we have exact flavor degeneracy; we then obtain a unique set of mass ratios. Although this mass spectrum is independent of the

number of flavors assumed, the results are in fact in good agreement with experiment for systems containing only u and d quarks.

Flavor-degeneracy breaking has to be introduced by hand. Once we have a mass difference such as $m_\psi - m_\rho$, however, we can calculate an entire set of other mass differences as well. One problem in the case of the heavy mesons is that we have less restrictive constraints, presumably a result of the fact that our dynamics is primarily the self-consistent dynamics of the flux tube joining the valence quarks, which is dominated by the light quarks. This results in a lack of uniqueness and to the need for extra conditions from a metastable string picture. It is nevertheless possible to find a very natural solution with minimum nonzero breaking of vector-pseudoscalar mass degeneracy which gives the masses of at least the low states for the different heavy-meson flavor families.

In the case of systems containing s quarks, we were able to obtain a unique light-meson mass-spectrum solution, given an arbitrary small positive K^*-ρ mass difference. Here the scale of flavor breaking is such that it is necessarily associated with small background contributions, rather than any systematic decoupling of states. The nature of such backgrounds must await calculations based on much more detailed models than the one we have been using here, but may well be associated with higher orders in the topological expansion, rather than the strictly planar level we have been assuming here. In particular, we have already seen, in Sec. V and Ref. 6, that the imposition of G parity on amplitudes which are assumed to be approximately planar leads to a breaking of π-η_{ud} mass degeneracy. But this means that, whereas we can only have the odd-G contributions π, ω,... to a in

$$\rho\rho(a)\pi\pi \to \alpha_\rho \,, \tag{8.1}$$

for example, we can also have the even-G contributions η_{ud}, ρ,... in

$$K^*K^*(a)KK \to \alpha_\phi \,. \tag{8.2}$$

We would therefore expect a higher effective s_a in the latter, which would lead, in turn, to a breaking of (ud)-s flavor mass degeneracy of the correct order of magnitude.

Our results are restricted to leading Regge trajectories and based on a number of approximations and assumptions concerning the role of secondary resonances and backgrounds. It would be straightforward, albeit technically difficult, to go beyond these approximations. For example, if we are to go beyond the peak approximation (3.14), we must explicitly tackle diagrams such as Fig. 2(b). This is discussed in more detail in Appendices B and C, and detailed calculations, at least at the simpler "zero-entropy" level, have been begun in collaboration with Nicolescu and Gauron. Ultimately, low-t backgrounds could be calculated by evaluating Eq. (3.7) for integer j. While it is unlikely that daughter trajectories will emerge from a [1,1] Padé approximant, they should arise from $[1,N]$ approximants with higher N. This would, of course, necessitate the evaluation of Figs. 2(c),....

In our simple scheme, we have used a version of duality based on the simple finite-energy sum rule (2.4). With a systematic program of calculations of the integer-j resonance and background contributions of the preceding paragraph, we could replace the δ-function term in Eq. (2.4) by a much more accurate expression for the low-s absorptive part, and, at the same time, progressively increase the value of $\bar{s}$, thereby obtaining an increasingly better version of this finite-energy sum rule.

Once we have a good representation of the planar level we could begin to tackle higher-order (nonplanar) terms in the topological expansion. In particular, the introduction of the cylinder (which corresponds to gluonium in QCD) should lead to large upward shifts of the η and η' masses, as argued several years ago by Millan.[14] It should also help to clarify the nature of gluonium, which is associated with a cylinder topology in the DTU scheme.

ACKNOWLEDGMENTS

The author would like to express his gratitude to Dr. B. Nicolescu for numerous helpful discussions and correspondences, to Professor G. F. Chew, Dr. P. Gauron, Dr. S. Ouvry, Dr. J. Kwiecinski, A. Morales-Acevedo, and E. Matute for valuable conversations, and to Professor R. Vinh-Mau for his hospitality at Laboratoire de Physique Theorique et des Particules Elementaires, Paris VI and Institut de Physique Nucleaire, Orsay, France, where part of this work was carried out. This work was supported in part by the U. S. Department of Energy.

APPENDIX A: A SIMPLIFIED PHYSICAL PICTURE OF OUR DYNAMICS

Let us consider a simplified version of our scheme in which we assume that only the lowest

nonvanishing contribution (a) dominates in Fig. 1(a), so that $s_0=\bar{s}$ in Eqs. (3.5) and (3.6). Now the peak approximation (3.14) is equivalent, at least in the immediate neighborhood of $j=\alpha$, to taking, for a given t,

$$G(y)=H(t)\delta(y-y_1),\quad y_1=\nu_1/\nu_a\ , \tag{A1}$$

which then gives

$$A_j=\frac{\Gamma(t)\nu_a{}^{-j-1}}{1-H(t)y_1{}^{-j-1}}\ . \tag{A2}$$

If we combine this with Eqs. (2.4), (3.10), (3.11), and the uniqueness of the leading output α for any given t, we are immediately led to Eq. (3.20). If, on the other hand, we expand the denominator of Eq. (A2), we obtain

$$A_j=\Gamma\nu_a{}^{-j-1}[1+Hy_1{}^{-j-1}+H^2y_1{}^{-2j-2}+\cdots]\ , \tag{A3}$$

which has the structure of a factorizable model.

Strictly speaking, Eq. (A3) need only be valid in the immediate neighborhood of $j=\alpha$. If we nevertheless take the inverse of the Mellin transform (3.3) (which involves an infinite range of j), we obtain

$$A(s,t)=\Gamma(t)[\delta(\nu-\nu_a)+H(t)\delta(\nu-\nu_a y_1)+H^2(t)\delta(\nu-\nu_a y_1{}^2)+\cdots]\ . \tag{A4}$$

If we introduce the variable

$$Y=\ln\nu\ , \tag{A5}$$

which reduces to the usual rapidity variable for large s, we see that the δ functions in Eqs. (A4) are equally spaced in Y, with a spacing

$$\Delta Y=\ln(\nu_1/\nu_a)\ . \tag{A6}$$

The nth term in the sum of Eq. (A4) or Fig. 2 can now be interpreted as an average representation of the contribution of an n-particle intermediate state to A, so that, in effect, we have an additional particle in the intermediate state every time we increase Y by the s-independent amount ΔY. This corresponds to the quark duality diagram of Fig. 9, which can be readily factorized into the pieces (i), (ii), (iii),. . ., at least if we make the usual kinematic approximations, justifying thereby the factorizable structure of both the coefficients and the positions of the δ functions of Eq. (A4).

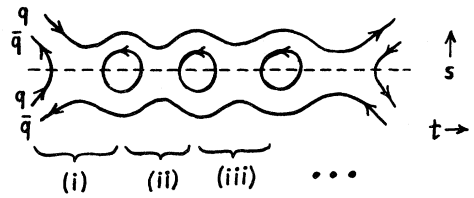

FIG. 9. Figure 1(b)-type quark-duality diagram displaying its factorizability into the pieces (i), (ii), (iii), . . . and the contribution of an n-hadronic-particle intermediate state, represented by the lines cut by the dashed line.

For $1=2$, $3=4$, and $t=0$, A is related, via the optical theorem, to the total cross section for $1+3\to$anything. The nth δ function can then be related, in an average sense, to the cross section for $1+3\to n$ particles, so that an additional particle is produced every time Y is increased by the s-independent amount ΔY. For large s, this gives rise, in an average way, to a multiplicity which grows logarithmically with s.

The above picture is, of course, just the familiar one which arises when we have jet formation in a high-s small-$|t|$ collision. As a final-state $q\bar{q}$ pair separates, it becomes energetically favorable for the connecting tube or string to break up and produce another $q\bar{q}$ pair. This process is then repeated until the typical spacing in the string approaches the typical hadronic size of about 1 fm (~ 5 GeV^{-1}). We then have a uniform rapidity distribution for the final-state hadrons, with an average rapidity spacing which is independent of s.

Although we had to use Eq. (A3) well away from $j=\alpha$ to derive Eq. (A4), it turns out that the latter bears an average-duality relationship with t-channel Regge exchange and should thus be a good average approximation of A anyway. To see this we use the finite-energy sum rule

$$\int_{\bar{\nu}_{n-1}}^{\bar{\nu}_n} d\nu[A-b_1b_2\nu^\alpha]\nu^{-S_1-S_2}=0\ , \tag{A7}$$

which is a generalized version of Eq. (2.4). The natural interval $\bar{\nu}_{n-1}<\nu<\bar{\nu}_n$ "occupied" by the $(n+1)$th δ function in Eq. (A4) would be one with

$$\bar{\nu}_n=F\nu_a y_1{}^n\ , \tag{A8}$$

where F is a fixed factor (~ 2). From Eqs. (A4), (A7), and (A8) we then have

$$\Gamma[Hy_1{}^{-S_1-S_2}]^n\nu_a{}^{-S_1-S_2}=\frac{b_1b_2}{\alpha+1-S_1-S_2}[F\nu_a y_1{}^n]^{\alpha+1-S_1-S_2}\left[1-\left[\frac{1}{y_1}\right]^{\alpha+1-S_1-S_2}\right]\ . \tag{A9}$$

Since the denominator of Eq. (A2) vanishes for $j=\alpha$, so that $H=y_1^{\alpha+1}$, we see that the n-dependent factors cancel out completely from both sides of Eq. (A7), which then reduces to a consistent n-independent equation

$$\Gamma=\frac{b_1 b_2}{\alpha+1-S_1-S_2}(\Gamma\nu_a)^{\alpha+1}F^{-S_1-S_2}\left[1-\left[\frac{1}{y_1}\right]^{\alpha+1-S_1-S_2}\right]. \tag{A10}$$

If we do not make the assumption that $s_0=\bar{s}$ in Eqs. (3.5) and (3.6), then Eqs. (3.7), (3.9), and (A1) would give a more complicated version of the expansion (A3), whose inverse Mellin transform would correspond to a modification of Eq. (A4) in which the peaks are partially smeared out in s or ν. Our basic conclusions should remain the same, however.

APPENDIX B: COUPLINGS

Our Regge-trajectory result (3.24), which we used as a generic formula for our mass calculations, was based on the peak approximation (3.14), which might be expected to arise in a wide class of models (see also Appendix C). On the other hand, a hadronic-coupling calculation necessarily involves a more detailed model. We shall sketch one such possible model here.

We shall begin by assuming that Fig. 3(a) does not begin to be canceled by Figs. 3(b),... until we attain relatively high values of s. This means that we can approximate Fig. 2(b) by Fig. 3(a) when we evaluate a_{2j}. We shall furthermore approximate the ladder exchanges in Fig. 3(a) by Regge exchange and assume that the [1,1] Padé approximant is already a good representation of Eqs. (3.7), so that Eq. (3.8) becomes

$$K(j)=\phi a_{2j}/a_{1j} \tag{B1}$$

with $\phi^2 a_{2j}$ given by Fig. 10.

In general the upper cutoff s_0 in Eq. (3.5) for the cluster $(a,\ldots)$ of Fig. 2(a) may not be the same as the corresponding cutoffs $\hat{s}_0$ in the clusters $(b,\ldots)$ and $(c,\ldots)$ of Fig. 2(b) or Fig. 10. However, it is always possible to find other processes for which the $s_0(t)$ should be the same as the $\hat{s}_0(t)$ coming into the process being considered; for example, s_0 for $\rho\rho\to\pi\pi$ should be the same as the $\hat{s}_0$ for $\pi\pi\to\pi\pi$ if $\alpha=\alpha_\rho$ in Fig. 10. We might, of course, have to consider more than one process at the same time.

To evaluate Fig. 10 for, say, $\pi\pi\to\pi\pi$, we must first relate the couplings of the different contributions in $(b,\ldots)=(c,\ldots)$ to each other. Suppose we approximate these by narrow peaks at $s=m_b^2$, $m_{b(1)}^2$, $m_{b(2)}^2$,... with, say, a spacing of $1/\alpha'$ between them. We then have the generalized finite-energy sum rules of Fig. 11, which, with $b=b(0)=\pi$, gives

$$\gamma_{\pi b\alpha}(t')\gamma_{\pi b\alpha}(t'')=\int_0^{\bar{\omega}_1}d\omega\,\gamma_{\pi\pi\alpha}(t)g(t',t'',t)\omega^{\alpha(t)-\alpha(t')-\alpha(t'')} \tag{B2}$$

and

$$\gamma_{\pi b(n)\alpha}(t',t)\gamma_{\pi b(n)\alpha}(t'',t)=\int_{\bar{\omega}_n}^{\bar{\omega}_{n+1}}d\omega\,\gamma_{\pi\pi\alpha}(t)g(t',t'',t)\omega^{\alpha(t)-\alpha(t')-\alpha(t'')}\theta(\hat{s}_0-s), \tag{B3}$$

where

$$\omega=s+\tfrac{1}{2}(t-2m_\pi^2-t'-t''), \tag{B4}$$

and $\bar{\omega}_n$ is the value of ω evaluated at $s=\bar{s}_n$, with $\bar{s}_n$ midway between $s_{b(n-1)}$ and $s_{b(n)}$ for $n\geq 1$.

The actual expression for $\phi^2 a_2$ is, in general, rather complicated. It simplifies considerably for $t=0$, however. If we make the narrow-peak approximation of the preceding paragraph for $s=m_b^2$, $m_{b(1)}^2$,... and $s=m_c^2$, $m_{c(1)}^2$,... we have

$$\phi^2 a_2(s,0)=\sum_{nn'}B_{nn'}(s,0)\theta(s-s_0), \tag{B5}$$

where we have added a step function to prevent the double counting of contributions which are already included in $\phi a_1(s,0)$, as given by Eq. (3.5), and where

$$B_{nn'}(s,0)=\frac{q_{nn'}}{16\pi\sqrt{s}}\int_{-1}^{1}dz'\left|\frac{\gamma_{\pi b(n)\alpha}(t',0)\gamma_{\pi c(n')\alpha}(t',0)}{\sin\pi\alpha(t')}\right|^2$$

$$\times\left|s-\tfrac{1}{2}(t'-m_{b(n)}{}^2-m_{c(n')}{}^2-2m_\pi{}^2\right|^{2\alpha(t')}\theta(\sqrt{s}-m_{b(n)}-m_{c(n')}) \tag{B6}$$

with $n,n'=0,1,2,\ldots$, $b(0)=b$, $c(0)=c$, $\bar{\omega}_0=0$,

$$4sq_{nn'}{}^2=[s-(m_{b(n)}-m_{c(n')})^2][s-(m_{b(n)}+m_{c(n')})^2] \tag{B7}$$

and

$$2t'=4q_{\pi\pi}q_{nn'}z'-(s-m_{b(n)}{}^2-m_{c(n')}{}^2-2m_\pi{}^2)\ . \tag{B8}$$

Since $b=c=\pi$, Eqs. (B2) and (B3) relate all of our couplings to $\gamma_{\pi\pi\alpha}(t)$, which can, in turn, be related to $\Gamma(t)$ through Eq. (2.4) with $b_1b_2=\gamma_{\pi\pi\alpha}{}^2$. The simplest approximation for $\Gamma(t)$ would be to assume that it is dominated by the $J^P=1^-\rho$ resonance. This would not, however, give rise to a nonsense wrong-signature zero at $\alpha(t)=0$ for $\gamma_{\pi b\alpha}{}^2(t')$, which is needed to cancel the pole arising at that point from the $\sin\pi\alpha(t')$ denominator in Eq. (B6). We must therefore add in just the right amount of a $J^P=0^+$ contribution of the same mass so that $\Gamma(t)\propto\alpha(t)$. This would not, of course, enable us to cancel the $\alpha(t)=-2,-3,\ldots$ poles arising from the same $\sin\pi\alpha(t')$ denominator in Eq. (B6), so we must insert a cutoff, say, at $\alpha(t')=-1.5$, to exclude them. The region $\alpha(t')<-1.5$ should give a negligible contribution to our integral, however.

One way of avoiding an $\alpha(t')=-1.5$ cutoff altogether is to relate $\Gamma(t')$ to $\gamma_{\pi\pi\alpha}(t')$ on the assumption that the $\pi\pi\to\pi\pi$ amplitude can be represented by the Lovelace-Veneziano model. Alternatively, we could assume a FESR where, instead of Eq. (2.4), we take the higher upper limit $\bar{s}=s_a+(N+\frac{1}{2})\alpha'^{-1}$ and include states at $s=s_a$, $s_a+\alpha'^{-1},\ldots s_a+N\alpha'^{-1}$. This means that we will have contributions with $J=0,1,\ldots,N+1$ which will give a polynomial in t' whose coefficients can be adjusted to give zeros in $\gamma_{\pi\pi\alpha}{}^2(t')$ at $\alpha(t')=0,-2,-3,\ldots,-(N+1)$; the FESR already gives a zero at $\alpha(t')=-1$ automatically. We would then not have any problem until we get to $\alpha(t')=-(N+2)$, so that we would only require a cutoff $\alpha(t')=-(N+\frac{3}{2})$.

Once we have an expression for ϕ^2a_2, we could use Eq. (3.10) and the condition

$$K'(\alpha)/K(\alpha)=-\ln(\nu_1/\nu_a)$$
$$=-(e-1)\ln(\bar{\nu}/\nu_a)\ , \tag{B9}$$

which follows from Eqs. (3.9), (3.14), and (3.19), as constraints to determine both $s_0=s_0(t)$ and the overall normalization of our coupling for any given t.

APPENDIX C: CORRECTION TO THE PEAK APPROXIMATION

The central dynamical approximation in our scheme is Eq. (3.14), which leads to Eq. (3.15) and becomes exact in the limit of an infinitesimally narrow $G(y)$ distribution in Eq. (3.13). We shall now see that it continues to be a good approximation even when we have a fairly broad distribution for $G(y)$.

We first note that, even if we do not make the approximation (3.14), Eq. (3.13) can be reduced to the form (3.15) provided c_1 is X dependent, with

$$c_1=c_1(X)=-\frac{1}{\ln\bar{y}}\left[\frac{K'(\alpha)}{K(\alpha)}+\ln\frac{y_0}{\bar{y}}\right]\ . \tag{C1}$$

Although the right-hand side of Eq. (3.15) is now no longer exactly linear in X, we could still impose

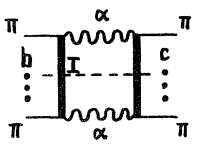

FIG. 10. Figure 3(a) for $\pi\pi\to\pi\pi$ in the Regge-exchange approximation.

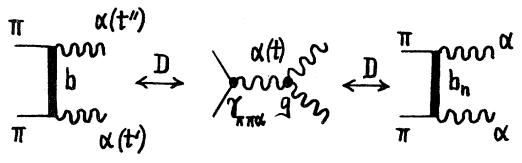

FIG. 11. Generalized finite-energy sum-rule duality of Eqs. (B2) and (B3).

an output α (or X) uniqueness requirement by insisting that $Y=c_1(X)X$ be tangent to $Y=e^X$. This gives, when combined with Eqs. (3.15) and (C1), the result

$$\ln\bar{y}=\frac{1}{\alpha+1-S_1-S_2}+\frac{\partial}{\partial\alpha}\ln\left[\frac{K'(\alpha)}{K(\alpha)}+\ln\frac{y_0}{\bar{y}}\right]. \tag{C2}$$

Note that the approximation (3.14) within Eq. (3.13), i.e., within $K'(\alpha)/K(\alpha)$, leads to a vanishing of the last term in Eq. (C2), which then reduces to Eq. (3.20). Even if we do not wish to make the approximation (3.14), we could, of course, still drop the last term in Eq. (C2) as the first step in an iterative solution of Eqs. (3.15), (C1), and (C2).

Suppose we now rewrite Eq. (3.9) for $j=\alpha$ in the form

$$K(\alpha)=\int_{y_0}^{\infty}dy\,y^{-\lambda}G(y){y_1}^{\lambda-\alpha-1}\left[1+\frac{y-y_1}{y_1}\right]^{\lambda-\alpha-1}, \tag{C3}$$

where $y^{-\lambda}$ is a weighting factor, with λ chosen so as to optimize the peaking of $y^{-\lambda}G(y)$. If we now expand the last factor of Eq. (C3) in powers of $(y-y_1)/y_1$, we obtain

$$K(\alpha)={y_1}^{\lambda-\alpha-1}[g_0+(\lambda-\alpha-1)g_1{y_1}^{-1}+\tfrac{1}{2}(\lambda-\alpha-1)(\lambda-\alpha-2)g_2{y_1}^{-2}+\ldots], \tag{C4}$$

where

$$g_n=\int_{y_0}^{\infty}dy\,y^{-\lambda}G(y)(y-y_1)^n. \tag{C5}$$

The first term in the expansion (C4) is, by itself, clearly equivalent to the peak approximation (3.14) within $K'(\alpha)/K(\alpha)$ and leads to Eq. (3.20). We can minimize corrections to this by choosing y_1 so that $g_1=0$, in which case Eqs. (C2) and (C4) reduce to

$$\ln\bar{y}=\frac{1}{\alpha+1-S_1-S_2}+\frac{g_2{y_1}^{-2}}{g_0\ln(y_0/\bar{y}y_1)}+\cdots. \tag{C6}$$

Since the last term in Eq. (C6) is only a first-order correction, we can use the lowest-order result (3.19) to simplify it. Equation (C6) then gives

$$\alpha+1-S_1-S_2\simeq\frac{1}{\ln\bar{y}}\left[1+\frac{g_2}{eg_0}(y_1\ln\bar{y})^{-2}\right]. \tag{C7}$$

To proceed further, we must take a specific form for $G(y)$. One such form, which takes into account the (finite-width) features of Fig. 4, would be

$$y^{-\lambda}G(y)=\text{constant},\quad -f(y_1-y_0)<(y-y_0)<f(y_1-y_0)$$
$$=0,\ \text{otherwise}, \tag{C8}$$

where f is then a measure of the fractional width of $G(y)$ relative to the "space" in y available to it. If we insert Eq. (C8) into Eq. (C5) and again use the lowest-order Eq. (3.19) in evaluating the first-order correction term, Eq. (C7) reduces to

$$\alpha(t)\simeq S_1+S_2-1+\frac{1}{\ln\bar{y}}\left[1-\frac{f^2}{3e}\left[\frac{1-\bar{y}^{e-1}}{\ln\bar{y}}\right]^2\right]. \tag{C9}$$

As in the case of Eq. (3.20), to which it reduces in the $f\to 0$ limit, Eq. (C9) has a spurious cut in the ν_a plane in the interval $0<\nu_a<-(\bar{s}-s_a)$, and reduces to the linear form (3.21) in a region sufficiently far from this region of invalidity, but this time with

$$c=-\tfrac{1}{2}+\frac{f^2}{6e}(e-1)^2,\qquad 2\hat{\alpha}'=(\tfrac{1}{2}-c)/(\bar{s}-s_a) \tag{C10}$$

instead of Eq. (3.22). From this we see that, even with $f=\frac{1}{2}$, which corresponds to a fairly large fractional width for $y^{-\lambda}G(y)$, c deviates by less than 10% from its value in Eq. (3.22).

APPENDIX D: FESR for $N\bar{N}\to\pi\pi$

We shall now see how the FESR (2.4) arises in the special case of $N\bar{N}\to\pi\pi$. We first note that the t-channel $N\bar{N}\to\pi\pi$ process can be described in the usual way by the πN amplitude,[11]

$$T=\bar{u}(q_1)[U+\tfrac{1}{2}\gamma\cdot(q_1+q_2)V]u(q_2), \tag{D1}$$

where $\bar{u}$, u, and q_1,q_2 are the wave functions and four-momenta of the nucleons involved and U and V are the invariant amplitudes. Instead of U and V it is often more convenient to deal with V and

$$U'=U+2M\nu V/(1-t/4M^2)\,, \tag{D2}$$

where M is the nucleon mass. V and U' are free of kinematic singularities and satisfy fixed-t dispersion relations. Their s-channel absorptive parts B and A' have the Regge behavior[11]

$$B=\eta\nu^{\alpha-1}\,, \tag{D3}$$

$$A'=\chi\nu^{\alpha}\,, \tag{D4}$$

so that we have the FESR's

$$\int_0^{\bar{\nu}}d\nu(B'-\eta\nu^{\alpha})\nu^{-1}=0\,, \tag{D5}$$

$$\int_0^{\bar{\nu}}d\nu(A'-\chi\nu^{\alpha})\nu^{0}=0\,, \tag{D6}$$

where

$$B'=\nu B\,. \tag{D7}$$

Since $S_1+S_2=1$ for $N\bar{N}\to\pi\pi$, Eq. (D5) corresponds to Eq. (2.4), while Eq. (D6) entails making the replacement $S_1+S_2\to S_1+S_2-1$, as in Eq. (2.7). The amplitudes involved in the two equations are different, although B' and A' are both proportional to ν^{α} for large s.

APPENDIX E: UNITARITY OF [1,N] PADÉ APPROXIMANTS

We will now show that, if the amplitude T satisfies the unitarity relation

$$T^{-1}-T^{*-1}=-2i\rho\,, \tag{E1}$$

where ρ is a phase-space factor, and T has an expansion

$$T=\phi t_1+\phi^2 t_2+\cdots+\phi^{N+1}t_{n+1}+\cdots\,, \tag{E2}$$

then its [1,N] Padé approximant will also satisfy Eq. (E1), where

$$[1,N]=\frac{P_1}{Q_N}=\frac{\phi p_1}{1+\phi q_1+\cdots+\phi^N q_N}\,, \tag{E3}$$

with $p_1,q_1,\ldots,q_N$ adjusted so that an expansion of Eq. (E3) in powers of ϕ reproduces the first $(N+1)$ terms of Eq. (E2). In particular, $p_1=t_1$.

Now, from Eq. (E2)

$$T^{-1}=\frac{1}{\phi t_1}\left[1+\phi\frac{t_2}{t_1}+\cdots+\phi^N\frac{t_{N+1}}{t_N}+\cdots\right]^{-1}$$
$$=\phi^{-1}t_1^{-1}+\tau_0+\phi\tau_1+\cdots+\phi^{N-1}\tau_{N-1}$$
$$+\cdots\,. \tag{E4}$$

Clearly the terms $\tau_0,\ldots,\tau_{N-1}$ can only be built out of $t_1,\ldots,t_{n+1}$; the $t_{N+1},\ldots$ terms can only contribute to terms of order $\geq\phi^N$ in Eqs. (E4). If we repeat the same procedure for $(P_1/Q_N)^{-1}$ we must then obtain, by construction, the truncated series

$$(P_1/Q_N)^{-1}=\phi^{-1}t_1^{-1}+\tau_0+\phi\tau_1+\cdots$$
$$+\phi^{N-1}\tau_{N-1} \tag{E5}$$

with exactly the same $t_1,\tau_0,\ldots,\tau_{N-1}$ as in Eq. (E4).

If we insert the expansion (E4) into Eq. (E1) we obtain, order by order,

$$t_1^{-1}-t_1^{*-1}=0\,, \tag{E6}$$

$$\tau_0-\tau_0^{*}=-2i\rho\,, \tag{E7}$$

$$\tau_n-\tau_n^{*}=0,\quad n\geq 1\,. \tag{E8}$$

From Eqs. (E5)–(E7) we then have

$$(P_1/Q_N)^{-1}-(P_1/Q_N)^{*-1}=-2i\rho\,, \tag{E9}$$

so that the [1,N] Padé approximant (P_1/Q_N) exactly satisfies the unitarity relation (E1).

APPENDIX F: REPRESENTATION FOR $K(j)$

In Sec. III we saw that the structure (3.9) follows trivially from Eq. (3.8) when we truncate the latter at $N=1$ with $s_0=\bar{s}$. We shall now argue that it also follows for any N and $s_0>\bar{s}$.

We shall begin by considering the first term in the series (3.8) which, using Eqs. (3.3) and (3.5), has the form

$$\phi\frac{a_{2j}}{a_{1j}}=\frac{1}{\Gamma}\frac{\int_{\nu_{t2}}^{\infty}d\nu\, a_2(s,t)(\nu/\nu_a)^{-j-1}}{1+\int_{\bar\nu}^{\nu_0}d\nu\, b_1b_2\nu^{\alpha}(\nu/\nu_a)^{-j-1}}$$

$$=\frac{1}{\Gamma}\int_{\nu_{t2}}^{\infty}d\nu\, a_2(s,t)\left[\frac{\nu}{\nu_a}\right]^{-j-1}\left\{1-\int_{\bar\nu}^{\nu_0}d\nu' b_1b_2\nu'^{\alpha}\left[\frac{\nu'}{\nu_a}\right]^{-j-1}+\left[\int_{\bar\nu}^{\nu_0}d\nu' b_1b_2\nu'^{\alpha}\left[\frac{\nu'}{\nu_a}\right]^{-j-1}\right]^2-\cdots\right\} \tag{F1}$$

with $\nu_{t2}=\nu_0$. We thus have to deal with products of integrals of the form

$$I_{12}=\int_{\nu_1}^{\infty}d\nu\, A_1(\nu,t)\left[\frac{\nu}{\nu_a}\right]^{-j-1}\int_{\nu_2}^{\infty}d\nu' A_2(\nu',t)\left[\frac{\nu'}{\nu_a}\right]^{-j-1}. \tag{F2}$$

If we introduce a new variable y, such that $\nu'=y\nu_a{}^2/\nu$, and interchange the order of integration, we obtain

$$I_{12}=\int_{y_L}^{\infty}dy\, H(y)y^{-j-1} \tag{F3}$$

with

$$y_L=\nu_1\nu_2/\nu_a{}^2 \tag{F4}$$

and

$$H(y)=\int_{\nu_1}^{y\nu_a{}^2/\nu_2}d\nu\frac{\nu_a{}^2}{\nu}A_1(\nu,t)A_2(y\nu_a{}^2/\nu,t)\,. \tag{F5}$$

The rapid convergence of the expansion of Eq. (F1), and hence the validity of Eq. (F3), is always guaranteed for sufficiently high j. Equation (F3) can then always be defined by analytic continuation for smaller j.

If we now repeatedly apply Eqs. (F2)–(F4) we see that all the terms in the series (F1) can be reduced to the form (F3), with thresholds

$$y_L=\nu_{t2}/\nu_a\ ,(\bar\nu/\nu_a)\nu_{t2}/\nu_a,(\bar\nu/\nu_a)^2\nu_{t2}/\nu_a,\ldots\,. \tag{F6}$$

Since $\bar\nu/\nu_a>1$ and $\nu_{t2}=\nu_0$, Eq. (F1) therefore has the representation (3.9) which is therefore valid for the [1,1] Padé approximant.

We can repeat the above procedure for a_{nj}/a_{1j} for any integer $n>2$. The only change is that we now have $\nu_{t2}\to\nu_{tn}>\nu_0$ in Eq. (F1), so that we again obtain the form (F3), but with the lowest threshold now at $y_L=(\nu_{tn}/\nu_a)>y_0$. Finally, if we apply Eqs. (F2)–(F4) repeatedly to

$$(a_{n_1j}/a_{1j})^{n_1'}(a_{n_2j}/a_{1j})^{n_2'}\cdots$$

with $n_c\geq 2$ and $n_k'\geq 1$, we find that we again obtain the form (F3), but with the lowest threshold now at

$$y_L=(\nu_{tn_1}/\nu_a)^{n_1'}(\nu_{tn_2}/\nu_a)^{n_2'}\cdots\,. \tag{F7}$$

Since $(\nu_{tn_2}/\nu_a)\geq y_0>1$, we conclude that the sum (3.8) must have the representation (3.9).

APPENDIX G: SINGULARITIES AT $\nu_a=0,\ -(\bar s-s_a)$

In Sec. III we saw that Eq. (3.20) had branch points at $\nu_a=0$ and $\nu_a=-(\bar s-s_a)$. We shall now argue that these branch points arise only because of the approximations we have made and are in fact spurious.

Suppose, instead of the Padé approximant given by Eqs. (3.7) and (3.8), we construct a [1,N] Padé approximant for

$$A_j^{(n)}(t)=A_j(t)-\phi a_{1j}(t)-\cdots-\phi^{n-1}a_{n-1,j}(t)\,, \tag{G1}$$

so that

$$A_j^{(n)}=\frac{\phi^n a_{nj}}{1-K_n(j)}\,, \tag{G2}$$

where

$$K_n(j)=\frac{\phi a_{n+1,j}}{a_{nj}}+\phi^2\left[\frac{a_{n+2,j}}{a_{nj}}-\left[\frac{a_{n+1,j}}{a_{nj}}\right]^2\right]+\cdots \tag{G3}$$

and

$$a_{ij}(t)=\int_{\nu_{ti}}^{\infty} d\nu\, a_i(s,t)\nu^{-j-1},\quad i\geq n\ , \tag{G4}$$

with $\nu_{ti}>\nu_{ti'}$, if $i>i'$. The output pole at $j=\alpha$ can then only arise from

$$K_n(j=\alpha)=1\ . \tag{G5}$$

Using arguments similar to the ones in Appendix F, $K_n(j)$ can be written as a sum of integrals of the form (F3), with thresholds at

$$y_L=\prod_H(\nu_{tH}/\nu_{tn})\ , \tag{G6}$$

where a given ν_{tH} may occur several times within the product (G5), and where $\nu_{tH}>\nu_{tn}$. Instead of Eq. (F1), for example, we have

$$\phi\frac{a_{n+1,j}}{a_{nj}}=\frac{1}{D_n(j)}\int_{\nu_{t,n+1}}^{\infty} d\nu\, a_{n+1}(s,t)\left[\frac{\nu}{\nu_{tn}}\right]^{-j-1}\ , \tag{G7}$$

where

$$D_n(j)=\int_{\nu_{tn}}^{\infty} d\nu\, a_n(s,t)(\nu/\nu_{tn})^{-j-1}$$
$$=D_n(j_0)[1+\epsilon_n(j)]\ , \tag{G8}$$

$$\epsilon_n(j)=[D_n(j)-D_n(j_0)]/D_n(j_0)\ , \tag{G9}$$

and j_0 is any convenient value of j. We can expand

$$D_n^{-1}(j)=D_n^{-1}(j_0)[1-\epsilon_n(j)+\epsilon_n^2(j)-\cdots] \tag{G10}$$

in Eq. (G7) and repeatedly apply Eq. (F2) to obtain an integral representation given by Eqs. (F3) and (G6); a similar procedure can be followed for any of the terms in Eq. (G3). The rapid convergence of the expansion (G10), and hence the validity of our integral representation (F3), is always guaranteed for sufficiently high j; Eq. (F3) can then always be defined by analytic continuation for smaller j.

Equation (G2) can be used to derive a formula similar to Eq. (3.12) where, instead of Γ, we have an expression involving an integral over $a_n(s,t)$. Such a formula will only involve integrals with limits of the type given by Eq. (G6). To obtain an analog to Eq. (3.13) which does not depend on the overall normalization of a_n we must introduce an extra duality constraint; Eq. (2.4) is, of course, one possibility, but a more appropriate alternative would be

$$\int_{L_n}^{H_n} ds[A(s,t)-b_1b_2\nu^{\alpha(t)}]\nu^{-S_1-S_2}=0\ , \tag{G11}$$

where the interval $L_n<s<H_n$ is one where the relative contribution of a_n to A is maximal. We then obtain an equation which can be solved for $\alpha(t)$, e.g., by iteration, starting with a linear $\alpha(t)$. We then find that the resulting $\alpha(t)$ will only have t singularities at

$$\nu_{L_n}=0\ ,\quad \nu_{H_n}=0\ ,\quad \nu_{tn}=0,\quad \nu_{tH}=0\ , \tag{G12}$$

where ν_{tH} corresponds, of course, to all the possible values that come into Eq. (G6). As we increase n, Eq. (G12) corresponds to lower and lower values of t relative to $\nu_a=0$, $-(\bar{s}-s_a)$. We conclude that the singularities in Eq. (3.20) at these latter two points are spurious.

[1]M. A. Shifman, A. I. Vainshtein, and V. I. Zakharov, Nucl. Phys. B147, 385 (1979); B147, 448 (1979); B147, 519 (1979).

[2]G. F. Chew and C. Rosenzweig, Phys. Rep. 41, 263 (1978).

[3]L. Montanet, G. C. Rossi, and G. Veneziano, Phys. Rep. 63, 149 (1980); R. Capella, B. Nicolescu, and J. Trân Thanh Vân, in *Low Q2 Physics*, proceedings of the XVIth Rencontre de Moriond, Les Arcs, France, 1981, edited by J. Trân Thanh Vân (Editions Frontieres, Dreux, France, 1981).

[4]G. Veneziano, Nucl. Phys. B74, 365 (1974); B117, 519 (1976); Phys. Lett. 52B, 220 (1974); Chan Hong-Mo, J. E. Paton, and Tsou Sheung Tsun, Nucl. Phys. B86, 479 (1975).

[5]G. F. Chew and V. Poenaru, Z. Phys. C 11, 59 (1981); Phys. Rev. Lett. 45, 229 (1980); H. Stapp, Lawrence Berkeley Laboratory Report No. LBL-10774, 1980 (unpublished).

[6]L. A. P. Balázs, Phys. Rev. D 20, 2331 (1979).

[7]L. A. P. Balázs, Phys. Lett. 71B, 216 (1977).

[8]L. A. P. Balázs and B. Nicolescu, Z. Phys. C 6, 269 (1980); Phys. Lett. 72B, 240 (1977).

[9]L. A. P. Balázs, Phys. Lett. 99B, 481 (1981).

[10]P. Gauron, B. Nicolescu, and S. Ouvry, Phys. Rev. D 24, 2501 (1981).

[11]P. D. B. Collins, *An Introduction to Regge Theory and High Energy Physics* (Cambridge University Press, Cambridge, England, 1977).

[12]L. A. P. Balázs, Phys. Rev. D 2, 999 (1970); Phys. Lett. 29B, 228 (1969).

[13]P. H. Frampton, *Dual Resonance Models* (Benjamin, Reading, Massachusetts, 1974).

[14]J. Millan, Phys. Rev. D 15, 2695 (1977).

[15]Y. Nambu, Phys. Rev. D 10, 4262 (1974); L. Susskind, Nuovo Cimento 69A, 457 (1970); P. Goddard, J. Goldstone, C. Rebbi, and C. Thorn, Nucl. Phys. B56, 109 (1973); A. Chodos and C. Thorn, *ibid.* B72, 509 (1974); C. G. Callan *et al.,* Phys. Rev. Lett. 34, 52 (1975).

[16]A. B. Kaidalov, Z. Phys. C 12, 63 (1982).